Applied Catalysis B: Environmental 164 (2015) 433–442

Contents lists available at ScienceDirect

Applied Catalysis B: Environmental

journal homepage: www.elsevier.com/locate/apcatb

Methane formation over TiO_2-based photocatalysts: Reaction pathways

Anna Cybula, Marek Klein, Adriana Zaleska*

Department of Chemical Technology, Gdansk University of Technology, 11/12 Narutowicza, 80-233 Gdansk, Poland

ARTICLE INFO

Article history:
Received 19 June 2014
Received in revised form 8 September 2014
Accepted 16 September 2014
Available online 28 September 2014

Keywords:
TiO_2
CO_2 photoconversion
Carbon ^{13}C
Reaction mechanism

ABSTRACT

The effects of organic impurities adsorbed or incorporated into semiconductors structure on the photocatalytic products are noteworthy. For this purpose, the as-prepared Ag, Au and Pd-modified TiO_2 samples were exposed to UV–vis irradiation in various gas atmospheres (CO_2, N_2, 600 ppm CO_2 in N_2, and $^{13}CO_2$) in order to clarify the route of CH_4 formation in the process of photocatalytic CO_2 reduction. In the presented research it was shown that in N_2 atmosphere the high concentration of methane was formed. For the removal of the organic adsorbates from photocatalysts the elongated calcination process was applied, however, it occurred insufficient for carbonless TiO_2 preparation. The highest amount of methane was formed in the presence of the 0.5Ag-TiO_2 sample which contained the highest amount of carbon. Experimental data, including isotope labelling results, confirmed that the obtained methane was formed from the organic impurities incorporated into TiO_2 structure and not from the $^{13}CO_2$.

1. Introduction

Photocatalytic reactions over solid semiconductors in the form of thin films or suspended nanoparticles (e.g. titanium dioxide) has been proposed as an environmental friendly process for treatment and purification of water and wastewater as well as the process for photoconversion of solar energy to hydrogen, methane and other low hydrocarbons (so called "artificial photosynthesis"). Recently, the possibility of methane formation have been reported during irradiation of CO_2-saturated aqueous solution containing suspended TiO_2 [1–5] and gas mixture of CO_2 with H_2O over TiO_2 [6–18]. Both pure [19–25] and modified TiO_2 [26–30] photocatalyst were used for CO_2 conversion into light hydrocarbons. Matejowa et al. [31] obtained gold-enriched TiO_2 and TiO_2-ZrO_2 *via* sol–gel method and tested as-prepared photocatalysts for the CO_2 photocatalytic reduction under the 254 nm UV-lamp. The photoactivity of investigated samples follows the order: TiO_2-ZrO_2 > Au/TiO_2-ZrO_2 > TiO_2 > Au/TiO_2 > TiO_2 Evonic P25. The authors stated that decreased photocatalytic activity of Au/TiO_2-ZrO_2 and Au/TiO_2 can be explained by the presence of large Au crystallites due to blocking the surface, reducing the light absorption capacity of the photocatalysts, or serving as the recombination centres. Koci et al. [32] examined Pd/TiO_2(-ZrO_2) nanoparticles in CO_2 photocatalytic reduction using a batch annular photoreactor. Methane and hydrogen were found as the main reduction products in the gas phase. They observed an unfavourable effect of Pd surface modification on the photocatalytic properties of TiO_2 and TiO_2-ZrO_2 samples probably due to the presence of PdO clusters, masking the supports surface resulted in reducing the light absorption ability of the Pd-photocatalysts. Furthermore, PdO clusters can work as recombination centres. Li et al. [33] tested CO_2 photocatalytic reduction in the gas phase over Pt, Au, Ag and nitrogen doped mesoporous TiO_2. Generally, they observed that noble metals loading enhanced photoactivity, and the efficiency follows the order: Pt > Au > Ag. The optimum loading amount of Pt was 0.2 wt.%.

On the other hand, it is well known that semiconductor particles with a large surface area show a tendency to adsorb organic contaminants on their surfaces and can contain organic impurities originated from reagents used during preparation. Both types of organic compounds might act as a carbon source for the products and as an electron donor and recently it has been demonstrated that methane produced during photoconversion process is also formed from the carbon adsorbed on the surface of the photocatalysts [34]. Yui et al. [34] showed that the calcination of TiO_2 can effectively reduce the amount of the organic adsorbates on its surface, however, re-adsorption of the organic compounds from air, during sample cooling to the room temperature, was observed. The additional sample treatment by means of rinsing with deionized water reduced the organic adsorbates content to the amount not exceeding the detection limit of each of them. To recognize the carbon source in methane production over Pd-TiO_2, GC–MS test using

* Corresponding author. Tel.: +48 58 347 24 37; fax: +48 58 347 20 65.
E-mail addresses: adriana.zaleska@pg.gda.pl, adriana.zaleska@ug.edu.pl (A. Zaleska).

http://dx.doi.org/10.1016/j.apcatb.2014.09.038
0926-3373/

$^{13}CO_2$ was performed [34]. Based on the presence of $m/e = 17$ peak presented at GC–MS chromatogram, authors stated that $^{13}CH_4$ was formed directly from $^{13}CO_2$. However, the $m/e = 17$ peak could be attributed both to the presence of $^{13}CH_4$, water vapour peak or noise detector. Additionally, the $m/e = 16$ peak was detected on the GC–MS spectra and assigned to the presence of $^{12}CH_4$, that was probably produced from the CO_3^{2-} species adsorbed on the photocatalysts [37]. However, $m/e = 16$ peak could be assigned both to the presence of $^{12}CH_4$ or $^{13}CH_4$ (defragmentation ion). Yang et al. [35] investigated the process of CO_2 photoconversion in the presence of Ti-SBA-15 and different gas mixtures. They found that since the Ti-SBA-15 was illuminated in the humid helium, the small amounts of ethane, methane and ethylene were formed [35]. Based on these results, it could be assumed that the observed hydrocarbons were formed from the carbon residues remaining from the precursor compounds used in the synthesis, however, the carbon origin have not been studied in this work. The small amount of methane (0.3 μmol g^{-1} cat h^{-1}) was also detected by Li et al. after irradiation of nitrogen over Pt-TiO_2 and assigned to methane produced from the carbon residues [36]. By using the combination of DRIFT spectroscopy and ^{13}C labeled CO_2, Yang et al. showed that the carbon residues significantly participate in the formation of CO over Cu-TiO_2 photocatalysts [37]. The isotope distribution of the adsorbed CO (^{12}CO at 2115 cm^{-1} and ^{13}CO at 2069 cm^{-1}) over Cu^I/TiO_2 was monitored. Adsorbed ^{12}CO species were found as the primary product, indicating that a reverse disproportionation reaction of the impurity carbon with labeled CO_2 proceeded, resulting in the CO formation. The authors also confirmed the presence of ^{13}CO, formed during the experiment, according to following reaction:

$$^{12}C\,(\text{impurity in/on catalysts}) + {}^{13}CO_2 \rightarrow {}^{12}CO + {}^{13}CO \quad (1)$$

The FTIR results did not constitute a sufficient evidence to prove or exclude artificial photosynthesis. The maximum peaks of $^{13}CO_2 + H_2O$ and $^{12}CO_2 + H_2O$ mixtures are almost identical, whereas the reason of shifting of the individual compounds maximum absorption is the presence of other substances in high concentration, particularly water.

Accordingly, it appears that only the confirmation of the ^{13}CO presence by means of GC–MS can absolutely ascertain that the process of CO_2 reduction proceeds. Based on the literature data and own investigation, it could be stated that carbon residues are formed in the surface layer and bulk of TiO_2 during the photocatalyst synthesis which often involves the use of organic solvents and organic TiO_2 precursors. The removal of these deposits by calcination in air is insufficient. In this work for the first time we have reported about the photoconversion process in the presence of TiO_2 modified with noble metals under UV–vis irradiation and with application of labeled carbon ^{13}C isotope in CO_2. Additionally, the photoconversion of CO_2/N_2 and CO_2/CH_4 gaseous mixture were carried out to clarify the route of hydrocarbon formation during photocatalytic CO_2 reduction over mentioned photocatalysts.

2. Experimental

2.1. Materials

Titanium(IV) isopropoxide (TIP) (97%) was purchased from Sigma-Aldrich and used as titanium source for the preparation of TiO_2 nanoparticles. $HAuCl_4$ (Au ~ 52%), $PdCl_2$ (5 wt.% solution in 10 wt.% HCl), potassium tetrachloroplatinate (II) from Sigma-Aldrich and silver nitrate (pure p.a.) from POCH S.A. Poland were used as metal source in the preparation procedure. Cyclohexane was used as the continuous oil phase, and sodium bis-(2-ethylhexyl) sulfosuccinate (AOT) purchased from Sigma-Aldrich as the surfactant, and aqueous solution as the dispersed phase, with addition of isopropyl alcohol as co-surfactant. Hydrazine (60%) were purchased from Sigma-Aldrich and used as the reducing agents. Ethyl alcohol was used as a solvent to prevent rapid hydrolysis of titanium alkoxide in sol–gel method. A commercial form of TiO_2 (P25, crystalline composition: 80% anatase, 20% rutile, surface area 50 g/m^2) from Evonik, Germany was used for the comparison of the photocatalytic activity. The labeled ^{13}C carbon isotope in CO_2 molecules was used as a substrate (^{13}C 99%, <1% ^{18}O from Cambridge Isotope Laboratories, Inc.).

2.2. Preparation of photocatalysts

2.2.1. Microemulsion method

Au/Pd-TiO_2, Au-TiO_2 and Pd-TiO_2 were obtained *via* microemulsion method described in our previous publication [38]. Au/Pd-TiO_2 was prepared by adding palladium precursor ($PdCl_2$) into water/AOT cyclohexane microemulsion A containing gold precursor ($HAuCl_4$). The water content was controlled by fixing the molar ratio of water to the surfactant at 2. Mixing was carried out for 1 h under nitrogen. Next the gold and palladium were reduced by dropwise addition of microemulsion B containing the reducing agent (hydrazine) and then TIP was added. The molar ratio of the reducing agent to metal ions equalled to 3. Microemulsion was mixed and purged with nitrogen for 24 h and then obtained precipitate was washed with acetone and water to remove the remaining surfactant. The obtained nanocomposites were dried at 80 °C and calcined at 400 °C for 3 h. Au-TiO_2 and Pd-TiO_2 photocatalysts were received by the same method but with the addition of one metal precursors ($PdCl_2$ or $HAuCl_4$) into microemulsion A. The molar ratio of water to the surfactant was 3 for TiO_2 modified with monometalic nanoparticles. Unmodified TiO_2, used as the reference material, was received by the same method but without the addition of metal precursors.

2.3. Sol–gel method

Anatase titanium dioxide nanoparticles were prepared by hydrolysis of TIP with water. TIP was mixed with ethanol and deionized water in specific proportions by volume ($V_{TIP}/V_{Ethanol} = 1$ and $V_{TIP}/V_{H_2O} = 1.75$). After addition water the white thick precipitate was formed. The mixture was stirred for 30 min using a magnetic stirrer to form clear sol. Then metal precursor ($AgNO_3$, K_2PtCl_4) was dissolved in deionized water at room temperature and mixed with TiO_2 gel. The mixture was stirred about 1 h at ambient temperature. The resulting gel was dried at 80 °C and then calcined from 2 to 10 h at different temperatures [39].

2.4. Measurement of photocatalytic conversion of carbon dioxide

In a typical measurement the photocatalysts powder was suspended in a small amount of water and loaded as a thick film on a glass plate (3 cm × 3 cm) using painting technique. The obtained TiO_2-coated support was dried for 20 h at 120 °C. Compressed gas (CO_2, N_2 or $^{13}CO_2$) was continuously bubbled through a thermostated water to bring a humid gas into the photoreactor. After purging with a mixture of gases, the valves on both sides of the reactor chamber were closed to seal the reactor and irradiated using 1000 W Xenon lamp (Oriel), emitting both UV and visible light. Measured light flux was (in the range from 310 to 380 nm) 62 mW/cm^2 for Xe lamp. The optical path included a 10 cm thick water filter to cut off IR. The photocatalysts activity tests were carried out in a flat stainless steel reactor with the working volume of about 30 cm^3 (see details in Fig. 1). The reactor was equipped with a quartz window, two valves and a septa.

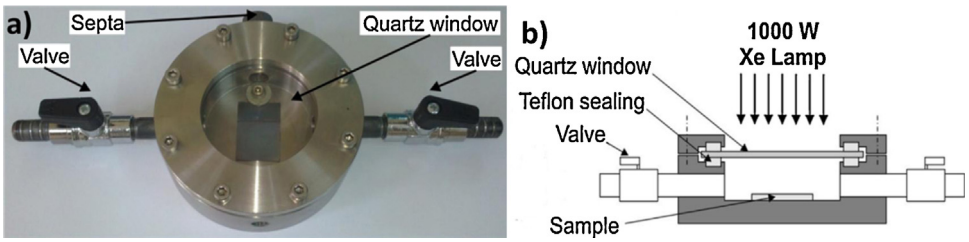

Fig. 1. Image of gas phase photoreactor (a) and scheme of photoreactor equipped with 1000 W Xe lamp as an irradiation source (b).

2.5. Gas chromatography analysis

Both, GC/FID and GC/MS were used to investigate the kinetics and mechanism of methane formation. A Perkin-Elmer modelClarus500 gas chromatograph was used together with a porapak-Q 100-120 mesh column (2 m × 2.1 mm i.d.) equipped with a flame ionization detector. In each case a 0.2 ml of gaseous sample was injected in a splitless mode. The operating conditions were as follows: the initial GC column temperature was 105 °C, and it was held so after injection for 10 min; the injector temperature was 150 °C while the detector temperature was 220 °C. Nitrogen was applied as the carrier gas at the constant flow of 17 cm^3 min^{-1}. The gas phase samples were withdrawn from the reaction chamber at given periods of time by the gas-tight membrane and analyzed in a duplicate. The retention time for methane, ethane and ethane was 0.74, 1.31 and1.58 min, respectively. A Perkin-Elmer model Clarus500gas chromatograph equipped with methanizer and FID detector was used together with a porapak-Q 100–120 mesh column (2 m × 2.1 mm i.d.) for the purpose of CO_2 content determination. The methane concentration in gas samples was calculated based on calibration curve, while the concentration of methane in calibration gas was 42 ppm.

To investigate the pathway of methane formation during irradiation of CO_2/H_2O over TiO_2, the GC/MS analysis was conducted. The labeled ^{13}C carbon isotope in CO_2 molecules was used as a substrate (^{13}C 99%, <1% ^{18}O). The GC/MS comprised of a Shimadzu GC-2010 gas chromatograph and QP-2010plus mass detector. The column (length: 30 m, diameter: 0.53 mm) was a Carboxen 1010 Plot column; from Supelco. The injector temperature was kept at 150 °C while the oven temperature was isothermal at 40 °C. Helium served as a carrier gas in a split mode (1:10). Column flow was 4.70 mL min^{-1}. The interface temperature was 220 °C whereas the ion source temperature was 200 °C. The MS was operated in a SIM mode, at 16 and 17 amu. The retention time for methane equalled to 4.35 min, while the detection limit was about 20 ppm in a SCAN mode and 5 ppm in a SIM mode. The methane peak of $m/e = 17$ attributable to $^{13}CH_4$ of the gas sample, produced by the photocatalytic reaction under a $^{13}CO_2$ atmosphere, was expected as a result.

3. Results and discussion

In a typical reaction, the CO_2 conversion is performed in a gas phase under UV–vis irradiation. Initially, we investigated the effect of photocatalysts type (pure and noble metals modified TiO_2) amount of metals, preparation method as well as calcination of temperature and time on the photoconversion CO_2 to hydrocarbons under $CO_2 + H_2O$ atmosphere (see Table 1). All the as-prepared TiO_2 samples loaded with noble metal nanoparticles, exhibited higher photoactivity than commercially available TiO_2 P25, which was chosen for this investigation as a standard used in heterogeneous photocatalysis. Methane was observed as the main products of CO_2 photoconversion. We also observed a small amount of ethene, ethane and methanol in the presence of 0.1Pd-TiO_2 and 1.25Au_0.5Pd-TiO_2 powders. The 0.25%Au-TiO_2, 0.25%Pd-TiO_2, 0.25%Au_0.25%Pd–TiO_2 samples (prepared by microemulsion method) and the 0.5%Ag-TiO_2 sample (prepared by sol–gel method) revealed the highest activity in methane formation under UV–vis irradiation among all tested photocatalysts and these sample were chosen for further examination. To investigate the effect of calcination temperature on the carbon residue and efficiency of methane formation, the 0.5%Ag-TiO_2 sample obtained by sol–gel method was additionally calcined at different times and temperatures.

3.1. Photocatalysts characterization

The BET surface area of the modified-TiO_2 samples, fluctuated from 91 to 182 m^2/g and was dependent on the type and amount of noble metal, calcination temperature and time as well as preparation method (see Table 2). The 0.25Pd-TiO_2 sample obtained by microemulsion method had the highest BET surface area of about 182 m^2/g. The 0.5 Ag-TiO_2 sample obtained by sol–gel method and calcined at 400 °C for 2 h had the lowest BET surface area of about 91 m^2/g. The samples modified with 0.25Au and 0.25Au_0.25Pd nanoparticles had BET surface areas of about 139 and 159 m^2/g, respectively. The presence and amount of silver, gold and palladium in the as-prepared photocatalysts was determined by X-ray Fluorescence (XRF) analysis and shown in Table 2. It was found that noble metal amount varied from 0.23 to 0.56 wt.%, depending on quantity of metal precursor introducing during sample preparation.

DRS spectra of TiO_2 modified with mono- and bimetallic nanoparticles and spectra of 0.5Au-TiO_2 calcined at different temperature (from 400 to 700 °C) and duration are shown in Fig. 2a and b, respectively. The spectra were taken using pure TiO_2 as a reference material. The results indicated that the visible light absorption of the TiO_2 samples was significantly improved by introducing the monometallic and bimetallic nanoparticles. It was found that for 0.25Pd-TiO_2 the diffuse reflectance spectrum shows a distinctive surface plasmon resonances (SPR) band at 432 nm. The band at ~440 nm (2.84 eV) could also be attributed to the d–d transition of PdO particles, that is, to the presence of PdO bulk phase [32]. For sample containing 0.25%Au, the characteristic SPR band and maximum is observed at 564 nm (see Fig. 2 and Table 2). For samples modified with Au/Pd nanoparticles we observed a wide band from 500 to 700 nm for Au nanoparticles with maximum in 548 nm. Kowalska et al. showed that absorption at 560–610 nm could be attributed to SPR of larger Au nanoparticles of about 30 to 60 nm [40]. It can be seen that Ag-TiO_2 nanoparticles calcined at the highest temperatures exhibit a well-defined absorption peak at 386 nm, which is consistent with the LSPR of silver metal particles with the size in the nanometer range, as was previously reported by us for Ag-TiO_2 nanocomposites [41]. It was observed that with decreasing calcination temperature this peak decreased and shifted toward longer wavelength. For the 0.5Ag-TiO_2 samples, calcined at 500 °C/10 h, 400 °C/10 h and 400 °C/2 h, the band maximum is observed at 383, 388, 401 nm, respectively. These results showed that with the decreasing of calcination temperature the

Table 1
Efficiency of hydrocarbon formation in the presence of various photocatalysts obtained by sol–gel and microemulsion method after 1 h exposure to UV–vis irradiation in $CO_2 + H_2O$ atmosphere. Experimental conditions: gas phase content: $CO_2 + H_2O$, irradiation source: 1000 W Xe lamp.

Type of photocatalyst	Amount of noble metal precursor [mol%]				Calcination temperature and time	Method of preparation	Photocatalysts amount [g]	The hydrocarbons concentration in the gas phase after 1 h exposure to UV–vis irradiation [ppm]			
	Au	Ag	Pd	Pt				Methane [ppm]	Ethene [ppm]	Ethane [ppm]	Methanol [ppm]
P25	0	0	0	0	–	–	0.045	2.6	<d.l.	<d.l.	<d.l.
Pure TiO_2	0	0	0	0	400 °C, 3 h	Microemulsion	0.082	3.6	<d.l.	<d.l.	<d.l.
0.1Au-TiO_2	0.1	0	0	0	400 °C, 3 h	Microemulsion	0.081	3.35	<d.l.	<d.l.	<d.l.
0.25Au-TiO_2	0.25	0	0	0	**400 °C, 3 h**	**Microemulsion**	**0.056**	**13**	<d.l.	<d.l.	<d.l.
0.1Pt-TiO_2	0	0	0	0.1	400 °C, 2 h	Sol–gel	0.037	3.7	<d.l.	<d.l.	<d.l.
0.1Pd-TiO_2	0	0	0.1	0	400 °C, 3 h	Microemulsion	0.160	11.6	2.2	3.5	9.6
0.25Pd-TiO_2	0	0	0.25	0	**400 °C, 3 h**	**Microemulsion**	**0.101**	**36**	<d.l.	<d.l.	<d.l.
0.5Ag-TiO_2	0	0.5	0	0	**400 °C, 2 h**	**Sol–gel**	**0.036**	**57**	<d.l.	<d.l.	<d.l.
0.1Pt_0.1Ag-TiO_2	0	0.1	0	0.1	400 °C, 2 h	Sol–gel	0.053	12	<d.l.	<d.l.	<d.l.
0.25Au_0.25Pd-TiO_2	0.25	0	0.25	0	**400 °C, 3 h**	**Microemulsion**	**0.134**	**65**	<d.l.	<d.l.	<d.l.
1.25Au_0,5Pd-TiO_2	1.25	0	0.5	0	400 °C, 3 h	Microemulsion	0.057	12.5	0.01	0.03	<d.l.

Table 2
Efficiency of methane formation in the gas phase over the various TiO_2-based photocatalysts irradiated in the $CO_2 + H_2O$ or $N_2 + H_2O$ atmosphere by UV–vis light and characterization of samples.

Atmosphere of the process	Type of photocatalyst [mol%]	Calcination temperature and time	Method of preparation	Methane concentration after 1 h exposure to UV–vis irradiation [ppm]		BET surface area [m^2/g]	Crystals size [nm]	Noble metal content determined by XRF analysis [wt.%]	LSPR[a] [nm]
				[ppm]	[ppm g^{-1}]				
CO_2	P25	–	–	2.6	57	50	–	–	–
N_2				1.3	37				
CO_2	0.25Au-TiO_2	400 °C, 3 h	Microemulsion	13	230	139	25.3	0.49 (Au)	574
N_2				19	163				
CO_2	0.25Pd-TiO_2	400 °C, 3 h	Microemulsion	36	356	182	36.7	0.26 (Pd)	432
N_2				48	466				
CO_2	0.25Au_0.25Pd-TiO_2	400 °C, 3 h	Microemulsion	65	486	159	19.3	0.59 (Au); 0.23 (Pd)	548
N_2				18	140				
CO_2	0.5Ag-TiO_2	400 °C, 2 h	Sol–gel	57	1580	91	12.4	0.45Ag	401
N_2				34	879				

[a] The maximum of main absorption peak.

size and shape of silver nanoparticles were changed. As the phase composition, crystallinity, and the crystallite size are important structural parameters which may correlate with the changes in the porous structure, they were investigated by using powder X-ray diffraction. Fig. 3 presents the results of XRD measurements for TiO_2 modified with Au, Pd or Au/Pd nanoparticles (Fig. 3a) and 0.5Au-TiO_2 calcined at different temperature (from 400 to 700 °C) and times (Fig. 3b). Typical diffraction peaks corresponding to anatase ($2\theta = 25.35°$, 37.78°, 47.5°, 53.92°, 62.72°, 68.99°) and brookite ($2\theta = 31°$) were observed in all the samples prepared by

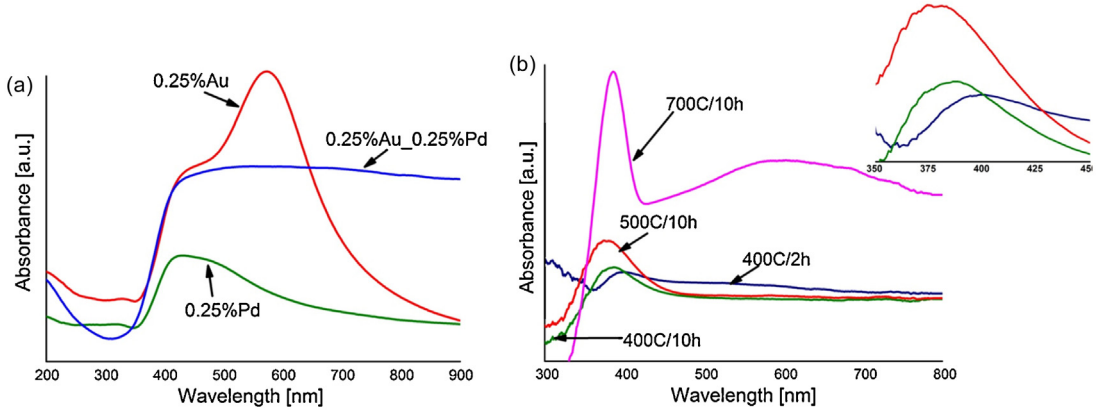

Fig. 2. DRS spectra of (a) 0.25Au-TiO_2, 0.25Pd-TiO_2, 0.25Au_0.25Pd-TiO_2 obtained by microemulsion method, (b) 0.5Ag-TiO_2 calcined at different temperatures and duration obtained via sol–gel route.

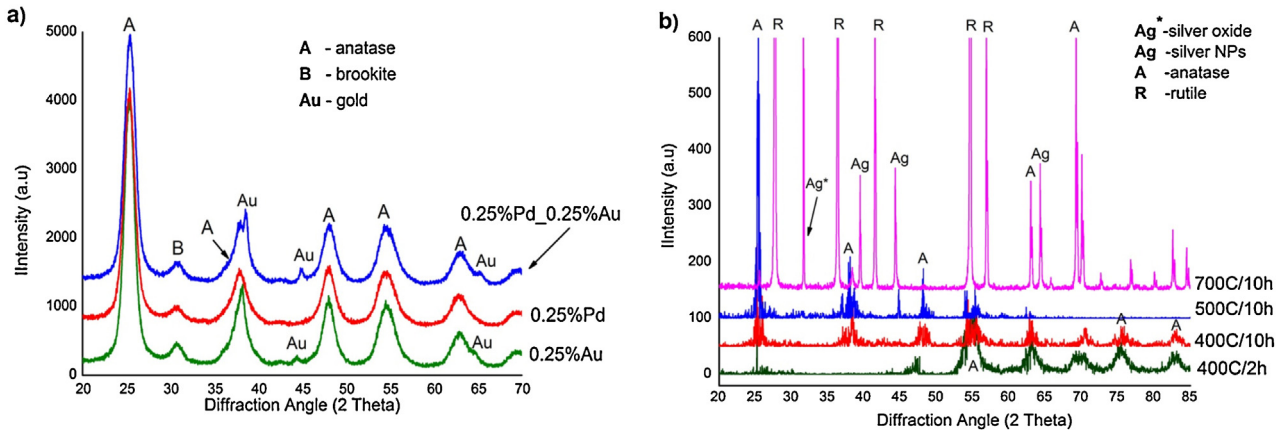

Fig. 3. XRD pattern of (a) 0.25Au-TiO_2, 0.25Pd-TiO_2, 0.25Au_0.25Pd-TiO_2 obtained by microemulsion method, (b) 0.5Ag-TiO_2 calcined at different temperatures and times obtained using sol–gel method.

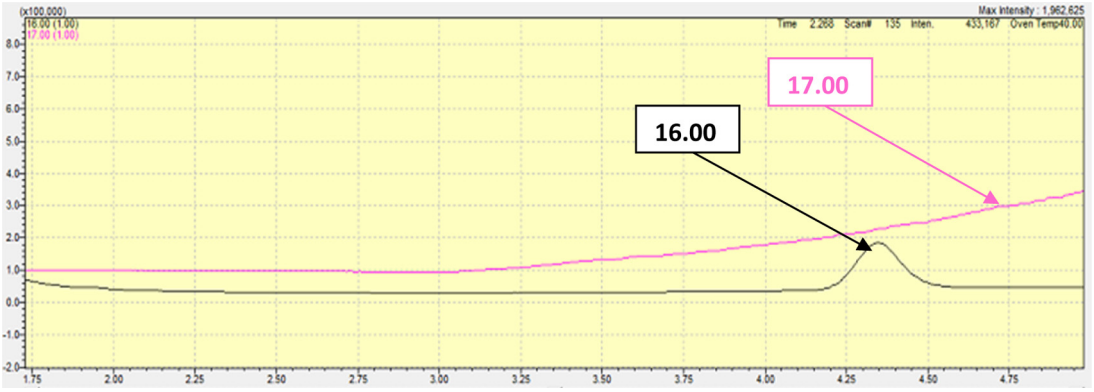

Fig. 4. Chromatogram of gaseous sample taking photoconversion process (in SIM mode at 16 and 17 amu). *Experimental conditions*: Gas phase content: $^{13}CO_2 + H_2O$, photocatalyst type: 0.5 mol% Ag modified-TiO_2 obtained by sol–gel method, photocatalyst amount: 0.037 g, irradiation source: 1000 W Xe lamp.

microemulsion method. Anatase is the major phase, whereas brookite exists as the minor phase. We observed for sample 0.25Au-TiO_2 and 0.25Au_0.25Pd-TiO_2 that peak originating from Au ($2\theta = 38.2, 44.4, 65.1^\circ$) [38]. We did not observe peaks related to the presence of Pd for samples Pd/TiO_2. An average particle size was determined on the base of Scherrer equations and equalled 25.3, 36.7 and 19.3 for 0.25Au-TiO_2, 0.25Pd-TiO_2 and 0.25Au_0.25Pd-TiO_2 samples, respectively (see Table 2). Fig. 3b illustrates the effects of calcination temperature and duration on the phase structure of the TiO_2 samples modified with 0.5 mol%. Ag and obtained by sol–gel method. Typical diffraction peaks corresponding to anatase ($2\theta = 25^\circ, 38^\circ, 48^\circ, 55^\circ, 63^\circ$) were observed for samples calcined at 400 and 500 °C. We did not observe peak related to the presence of silver nanoparticles for these samples probably due to weak intensity of these peaks. Zielińska et al. showed that the major phase of Ag-TiO_2 prepared using sol–gel method and calcined at 450 °C were anatase and brookite exists as the minor phase [39]. For sample Ag-TiO_2 calcined at 500 °C we do not observed reflexes from anatase in the range 70–85°. It can be seen that the intensity of the peaks increases at 700 °C and reflections attributed to rutile appeared ($2\theta = 27.4^\circ, 36.0^\circ, 41.3^\circ, 54.3^\circ, 56.6^\circ$). Only for sample calcined at the highest temperature we observed intense peaks attributed to silver. Diffraction peaks located at around 38.4°, 44.2° and 64.3° are corresponding to lattice plane reflections of Ag nanocrystals. Moreover, diffraction peaks at 31.6° could be assigned to the peaks of silver oxides (AgO and Ag_2O) formed during the oxidative etching process in contact with air [39].

3.2. The effect of sample type on the efficiency of methane formation

The methane concentration in the gas phase was measured to evaluate the efficiency of CO_2 photoconversion into light hydrocarbons in the presence of various TiO_2-based photocatalysts under UV–vis irradiation (see details in Table 2). Preparation of photocatalyst thin coatings at the surface of glass plates resulted in fixing of various amount of samples due to different surface area, particles size and adhesive properties of modified TiO_2. Therefore, for better understanding of presented results, the amount of fixed photocatalyst is also given in Table 2 and efficiency of methane formation was additionally calculated for 1 g of photocatalyst. The results show that methane is produced both after irradiation of TiO_2-based photocatalyst in the atmospheres containing CO_2 and after irradiation in the inert gas atmosphere. It means that at least part of methane originated from carbon species incorporated into photocatalysts structure. Generally, higher amount of methane was observed after irradiation of modified TiO_2 in the mixture of CO_2 and H_2O vapour than after irradiation of TiO_2 in nitrogen atmosphere. Only in case of the 0.25%Pd-TiO_2 sample amount of methane formed under CO_2 atmosphere was lower than that formed under N_2 one and equalled to 356 and 466 ppm g^{-1}, respectively. The lowest amounts of methane were formed in the presence of commercial TiO_2 (P25), both under CO_2 and N_2 atmospheres, which amounted to 57 and 37 ppm g^{-1}, respectively. Whereas, the highest amounts of methane were obtained in the presence

Table 3
The effect of calcination temperature and duration of the 0.5Ag-TiO_2 sample on the efficiency of methane formation in the CO_2 and N_2 atmosphere.

Atmosphere of the process	Type of sample	Temperature and time of calcination	Method of sample preparation	Photocatalysts amount [g]	Methane concentration after 1 h exposure to UV–vis irradiation	
					[ppm]	[ppm g^{-1}]
CO_2	0.5Ag-TiO_2	Without calcination	Sol–gel	0.044	591	13,328
N_2				0.038	30	790
CO_2	0.5Ag-TiO_2	400 °C, 2 h	Sol–gel	0.036	57	1580
N_2				0.038	34	879
CO_2	0.5Ag-TiO_2	400 °C, 10 h	Sol–gel	0.038	16	420
N_2				0.032	37	1155
CO_2	0.5Ag-TiO_2	500 °C, 10 h	Sol–gel	0.088	14	159
N_2				0.041	10	241
CO_2	0.5Ag-TiO_2	700 °C, 10 h	Sol–gel	0.082	15	184
N_2				0.125	7	56

of the 0.5%Ag-TiO_2 sample, obtained by sol–gel method and calcined for 2 h, for which the CH_4 concentration in the CO_2 and N_2 atmosphere were equalled to 1580 and 879 ppm g^{-1}, respectively. It could be expected that samples prepared by microemulsion method or sol–gel method contained carbon traces originated from titania organic precursor and microemulsion system (cyclohexane and surfactant). Thus, prolonged calcination time or enhanced temperature could be used to remove carbon impurities. Consequently, this sample was chosen to investigate the effect of calcination temperature and duration on the efficiency of methane formation. The 0.5Ag-TiO_2 photocatalyst was calcined up to 700 °C and up to 10 h to remove carbon impurities from which the methane could be formed. As expected, the highest methane production was observed in the presence of photocatalyst which was not subjected to calcination in CO_2 atmosphere, for which after 1 h of irradiation up to 13,328 ppm g^{-1} of methane was formed (see details in Table 3). Increasing temperature and duration of calcination step resulted in decrease of methane amount formed during irradiation of the 0.5Ag-TiO_2 sample in the CO_2 atmosphere. Methane concentration decreased from 1580 to 184 ppm g^{-1} for 400 °C_2 h and 700 °C_10 h samples, respectively. The lowest amount of formed methane (56 ppm g^{-1}) was recorded during the process carried out in the absence of CO_2 (N_2 atmosphere) for sample calcined in 700 °C. Whereas, in case of sample calcined in 500 °C amount of methane formed under CO_2 was lower than in the atmosphere of N_2 and amounted to 420 and 1155 ppm g^{-1}, respectively. For Ag modified-TiO_2 calcined in 400 °C for 10 h the amount of methane formed under CO_2 was also lower than that obtained in the atmosphere of N_2 (420 and 1155 ppm g^{-1}, respectively). These results indicate that the long high-temperature calcination is not a sufficient way for the complete removal of carbon from the TiO_2 surface. Additionally, these results suggested that methane is rather formed from carbon impurities and methane amount is rather dependent on carbon impurities availability, i.e. amount and chemical character of carbon impurities present at the surface of photocatalysts.

3.3. The effect of gas phase composition on the efficiency of methane formation

To investigate the origin of methane formed during irradiation of CO_2 mixture over the 0.5%Ag-TiO_2 sample, CO_2 labelled with ^{13}C carbon isotope was used in next experiment. The attributable to $^{13}CH_4$ methane peak of $m/e = 17$ of the gas sample produced by the photocatalytic reaction under a $^{13}CO_2$ atmosphere was expected as a result. However, in the course of research the signal at $m/e = 17$ was not obtained, only the $m/e = 16$ peak attributed

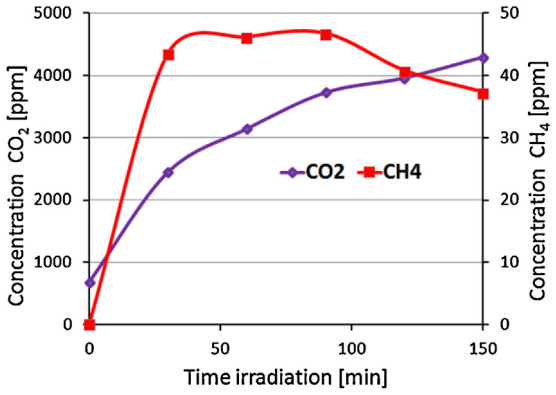

Fig. 5. Concentration of CO_2 and CH_4 in the gas phase during irradiation of $CO_2 + N_2 + H_2O$ mixture over 0.5%Ag modified-TiO_2. *Experimental condition*: Gas phase content: 600 ppm CO_2 in $N_2 + H_2O$, photocatalyst type: Ag modified-TiO_2 (0.5 mol% of Ag); photocatalyst amount: 0.061 g, irradiation source: 1000 W Xe lamp.

to $^{12}CH_4$ was recorded (see details in Fig. 4). This confirms that obtained methane was formed not from the $^{13}CO_2$ as expected but from the organic impurities incorporated into structure of photocatalysts. The signal-to-noise ratio at 16 amu was 61.47. To better understand the mechanism of reactions occurred at the surface of Ag-TiO_2, concentration of both, CO_2 and methane, was monitored in the gas phase. Due to the fact that chromatographic measurement is burdened with around 5% uncertainty, the CO_2 concentration had to be much lower than 99%. Therefore, for next experiments the standard mixture of 600 ppm CO_2 in N_2 (higher CO_2 concentration than that in the atmosphere) was prepared and used for further experiments with the 0.5%Ag-TiO_2 samples (see details in Fig. 5). The decrease in CO_2 concentration during the CH_4 generation would indicate that methane is formed from CO_2. Obtained results clearly pointed out that irradiation of gas mixture containing 600 ppm of CO_2 in the nitrogen over Ag-TiO_2 photocatalysts, resulted in increase of CH_4 concentration with simultaneous increase of CO_2 concentration. Thus, this study showed that during the process both CO_2 and CH_4 were formed. The CO_2 concentration was increasing rapidly during irradiation to reach after 150 min the level of about 3612 ppm. It may evidence that the oxidation of the carbon compounds, presented in the surface layer of photocatalysts surface, have occurred. Whereas, the CH_4 concentration increased rapidly at the beginning of the process and after 30 min of irradiation equalled to 43.5 ppm. Later on after 100 min of irradiation in the presence 0.5%Ag-TiO_2 sample the CH_4 concentration

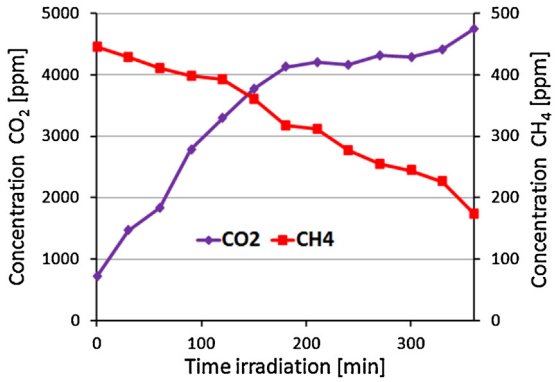

Fig. 6. Concentration of CO_2 and CH_4 in the gas phase during UV–vis irradiation of the 0.5% Ag modified-TiO_2 in the atmosphere containing CO_2, CH_4, H_2O and N_2. *Experimental conditions*: Gas phase composition: 715 ppm CO_2 in N_2 + 445 ppm CH_4 + H_2O, photocatalyst type: 0.5%Ag modified-TiO_2, photocatalyst amount: 0.039 g, irradiation source: 1000 W Xe lamp.

slightly decreased and finally after 150 min it reached 37.4 ppm. In next experiments, the gas mixture containing initially methane, carbon dioxide and water vapour dissolved in nitrogen, was used. Fig. 6 presents the concentration of CH_4 and CO_2 during irradiation of $CH_4 + CO_2 + H_2O + N_2$ (445 ppm CH_4 and 715 ppm CO_2) in the presence of the 0.5%Ag-TiO_2 sample. Obtained results showed that the concentration of CO_2 was increased rapidly during irradiation process since methane concentration decreased. 360 min of irradiation resulted in CO_2 concentration increased from 715 to 4747 ppm, when the amount of CH_4 gradually decreased from 445 to 174 ppm. It pointed out that preferred reaction direction is reaction of methane oxidation towards carbon dioxide instead of CO_2 reduction towards hydrocarbons and it clearly indicated that observed methane is formed due to oxidation of carbon impurities adsorbed on the photocatalyst surface.

Based on data presented in Table 2 and Figs. 5 and 6, it could be concluded that methane are formed and consumed at the same time during irradiation over TiO_2. Therefore, observed methane concentration resulted from competition of two processes: methane formation and methane oxidation and rate of both reactions are probably affected by type of the photocatalyst. Thus, observed lower concentration of methane formed over the 0.25Pd-TiO_2 sample under CO_2 atmosphere compared to N_2 atmosphere could be a result of higher rate of methane consumption at this stage of reaction comparing with other types of modified TiO_2.

3.4. Thermo-gravimetric and elemental analysis of TiO_2-based photocatalysts

All as-prepared samples modified with the noble metals were synthesized using sol–gel and microemulsion methods. To characterize them and determine carbon compounds working as methane precursors during UV–vis irradiation, elemental analysis and thermo-gravimetric analysis (TGA) were used. TGA can provide information about desorption, dehydration, oxidation or decomposition of samples. Thus, TGA was applied in order to determine the amount of water and organic adsorbents on the TiO_2 surface. The mass loss was measured for selected samples upon heating to 700 °C and presented in Fig. 7. The results showed that the samples weight decreased up to 90% with the increase of the calcination temperature. The highest weight loss was observed during the heating up to 200 °C. Probably adsorbed water was removed in the step. Additionally, the carbon content in photocatalysts was determined by elemental analysis. The carbon content varied from 0.014 to 0.21 wt.% of samples and it originated from the reagents used during the synthesis (surfactant, TiO_2 and metals precursors, reducing agent and the oil phase) and even adsorbates from atmosphere (see details in Table 4). As expected, the sample contained the highest amount of carbon (0.2051 wt.%) was responsible for higher methane production during UV–vis irradiation, while the sample of commercially available TiO_2 (P25), contained the lowest carbon content (0.0138 mass%), was liable for lowest methane concentration in the gas phase (see details in Tables 3 and 4). However, the 0.25Pd-TiO_2 sample, containing medium amount of carbon (0.0383 wt.%), shown highest activity in methane production among all sample obtained by microemulsion method. As it was mentioned before, it could be expected that observed methane concentration is affected not only by carbon content, but also carbon chemical character and surface availability. The 0.25Pd-TiO_2 sample revealed the highest surface area, therefore well developed surface area could favor converting of carbon species incorporated into surface layer into methane. The 0.25%Au/TiO_2 and 0.25%Pd/TiO_2 samples contained 0.0624 and 0.0383 mass % of carbon, respectively.

Maximum amount of theoretically formed CH_4 by transformation of carbon species incorporated into photocatalysts mass was calculated and presented in Table 4 and Fig. 8. To calculate the theoretical amount of methane, the mass of carbon incorporated into sample was converted to the number of moles and then to the quantity of methane. The results showed that the observed amount of CH_4 formed in the gas phase is much lower than theoretically calculated amount of CH_4. However, 60 min of UV–vis irradiation could be not enough to transform all carbon species into methane. On the other hand, carbon compounds are probably distributed in bulky material of TiO_2 and in the beginning of irradiation process, only carbon compounds incorporated into surface layer or adsorbed at the surface of TiO_2 could be transformed into methane. Although, we did not observe clear correlation between carbon content and methane amount determined in the gas phase for all investigated samples, however, samples containing the lowest (P25) and the highest (0.5Ag-TiO_2) amount of carbon revealed lower and higher activity in methane formation, respectively. Additionally, the

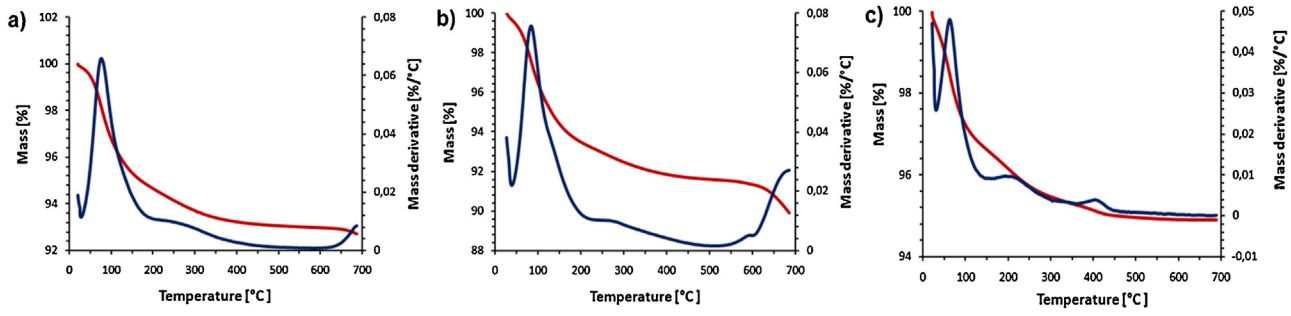

Fig. 7. The TGA thermal curves of sample: (a) 0.25Au-TiO_2, (b) 0.25Pd-TiO_2 and (c) 0.5Ag-TiO_2 calcined at 400 °C.

Table 4
Theoretically calculated and observed methane concentration formed over UV–vis irradiated photocatalysts related to carbon amount incorporated in samples.

Gas phase composition	Type of photocatalyst	Methane concentration after 1 h exposure to UV–vis irradiation		Photocatalysts amount [g]	Carbon content [wt.%]	Theoretical amount of CH_4 [a]
		[ppm]	[ppm g^{-1}]			[ppm]
CO_2	P25	2.6	57	0.045	0.0138	371
N_2		1.3	37	0.035		286
CO_2	0.25Au-TiO_2	13	230	0.056	0.0624	2077
N_2		19	163	0.116		4283
CO_2	0.25Pd-TiO_2	36	356	0.101	0.0383	2281
N_2		48	466	0.103		2323
CO_2	0.25Au_0.25Pd-TiO_2	65	486	0.134	0.0521	4103
N_2		18	140	0.129		3944
CO_2	0.5Ag-TiO_2	57	1580	0.036	0.2051	4357
N_2		34	879	0.038		4672

[a] Theoretical amount of methane was calculated as a maximum methane concentration formed from carbon incorporated into photocatalyst.

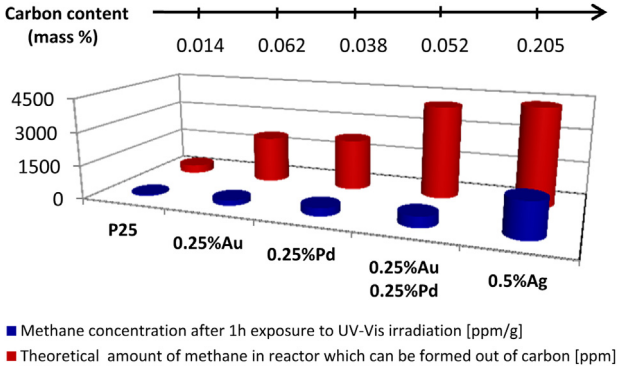

Fig. 8. Methane concentration after 1 h exposure to UV–vis irradiation and theoretical calculations of the amount of CH_4 in reactor ($V = 30\,cm^3$) which can be formed out of carbon.

photocatalysts containing the highest amount of carbon clearly showed better activity and the P25 sample, contained lower amount of carbon (0.0138 mass %) also showed the lowest activity in photoconversion process.

3.5. Mechanism discussion

As reported by Jiang et al., the properties of the potential photocatalysts are established by the redox potentials of the rate-limiting steps [42]:

(1) water oxidation: $2H_2O(l) \rightarrow O_2(g) + 4H^+(aq) + 4e^-$ $E^0_{ox} = -1.23$ V
(2) carbon dioxide reduction: $CO_2(aq) + e^- \rightarrow CO_2^-(aq)$ $E^0_{red} = -1.65$ V

On the other hand, the value of electrochemical potential of the reaction of single electron reduction of CO_2 to an anion radical ($CO_2^{\bullet -}$) is −1.90 V versus to normal hydrogen electrode [43]. Thus, these values dictate a minimum threshold for the energy of photo-excited electrons stipulated to reduce CO_2 molecule and also the energy levels of the conduction and valence bands of photocatalysts. According to summary of semiconductors properties presented by Habisreutinger et al., non of semiconductors provides adequate potential to transfer a single photogenerated electron to a free CO_2 molecule making this step highly impossible [43]. Thus, the reaction pathway for the CO_2 reduction with water should be cautiously investigated in order to establish whether the CO_2 from the gas phase really acts as a carbon source. The major obstacle for the reduction of CO_2 is the thermodynamic limitation.

$$CO_2(g) + 2H_2O(g) \rightarrow CH_4(g) + 2O_2(g), \quad (2)$$

$$\Delta G_r^\circ = +800.78 \text{ kJ mol}^{-1}$$

This significant up-hill free-energy change is due to the greater enthalpies for CO_2 and H_2O. The free-energy change for water splitting is lesser by 43%.

$$2H_2O(g) \rightarrow 2H_2(g) + O_2(g), \quad (3)$$

$$\Delta G_r^\circ = +4572 \text{ kJ mol}^{-1}$$

Therefore, also in view of the free-energy change, the CO_2 conversion is extremely unfavorable, and the reduction of impurity carbon to methane could be misinterpreted as the reaction of CO_2 [44]. Summarizing, the observed activity of studied TiO_2 samples in CO_2 photoconversion process into methane probably is mostly affected by the preparation route and resulted carbon content and type or carbon species in samples. It could be expected that one of the important parameter influenced efficiency of methane formation is also surface area of TiO_2-based photocatalysts. The specific surface area could determine the available surface active sites for the reaction to take place. Moreover, it could be responsible for amount of organic adsorbated seated at the surface of TiO_2 as well as for availability and reaction susceptibility of organic impurities incorporated into surface layer of TiO_2. Thus, to could be expected

that sample with well developed surface area and containing higher amount of carbon impurities in surface layer can show higher activity in methane formation and methane under UV–vis light. According to this theory, the sample 0.25Pd-TiO_2 having high surface area (182 m^2/g) and containing about 0.04 wt.% of carbon, produced quite high amount of methane (356 and 466 ppm g^{-1} for CO_2 and N_2 atmosphere, respectively). Nevertheless, it was found that the 0.5Ag-TiO_2 sample obtained by sol–gel method and calcined at 400 °C for 2 h had the lowest BET surface area whilst revealed the highest efficiency in methane generation. In this case, observed activity in methane formation of this sample is rather resulted from high carbon content, because short time and low temperature of calcination step was not enough to remove of the organic adsorbates and/or impurities. In fact, this sample contained the highest amount of carbon (0.2 wt.%) among all investigated samples. It could be noticed that the increase in temperature and duration of calcination step led to decrease of methane formation efficiency. It was shown in our previous study, that the photocatalysts containing more carbon species are able to create carbon radicals under UV–vis irradiation [38]. Low activity of TiO_2 Evonic P25 can be attributed to both, too large anatase crystallite size and the presence of rutile phase since the anatase crystallite size plays the key role in the photocatalytic reactions [31].

In our study in the presence of the 0.25Pd-TiO_2 sample prepared by microemulsion method and 0.5Ag-TiO_2 obtained by sol–gel system and calcined in 400 °C for 10 h, the amount of methane formed under CO_2 was lower than that obtained in the atmosphere of N_2. This phenomenon can be explained by competition of two processes: methane formation and methane oxidation during irradiation over modified TiO_2. The rate of both reactions is probably affected by type of the photocatalyst. Thus, observed lower concentration of methane formed over 0.25Pd-TiO_2 and 0.5Ag-TiO_2 under CO_2 atmosphere compared to N_2 atmosphere could be a result of higher rate of methane consumption at this stage of reaction comparing with other types of modified TiO_2. It is not clear at this moment how noble metals affected reaction of methane formation and oxidation. Noble metals doped or deposited on the surface of TiO_2 are expected to show various effects on the photocatalytic activity of TiO_2 by different mechanisms. They may (i) enhance the electron–hole separation due to Schottky barrier formation, (ii) extend the light absorption into a visible range and enhance surface electron excitation by plasmon resonances excited by visible light and (iii) modify the surface properties of photocatalysts [45].

4. Conclusions

In summary, the pathway of methane formation in the presence of TiO_2 modified with noble metals (Ag, Au and Pd) prepared by the microemulsion and sol–gel method was reported for the first time. Photocatalysts were exposed to irradiation in the presence of different gases (CO_2, N_2, CO_2/N_2, $CO_2/CH_4/N_2$ and $^{13}CO_2$) in order to explain the route of hydrocarbons formation in the process of CO_2 photoirradiation. We observed that in the N_2 atmosphere methane was formed in high concentration. The highest amount of methane was obtained in the presence of the 0.5Ag-TiO_2 sample which also contained the highest amount of carbon (~0.2 wt.%). After 1 h of light exposure in the presence of Ag-TiO_2 (0.5 mol.% of Ag) in N_2 atmosphere the amount of 879 ppm of methane was formed. In order to remove the organic impurities incorporated or adsorb at the photocatalysts surface the elongated calcination process was applied. It was observed that with the increasing temperature and duration of calcination the efficiency of methane formation under CO_2 and N_2 atmosphere decreased. Increasing calcination temperature from 400 to 700 °C during calcination step, causes decrease in methane concentration for reaction carried out in CO_2 atmosphere from 420 to 184 ppm g^{-1}, respectively. The calcination of samples can effectively reduce the amount of carbon species incorporated into TiO_2 structure and adsorbates from TiO_2 surface, however, this procedure is not enough to eliminate whole carbon from samples.

In order to confirm the formation of CH_4 from carbon impurities the process in the presence of 0.5Ag-TiO_2 and CO_2 labeled with ^{13}C carbon isotope was carried out. Experimental data, including isotope labelling, confirmed that methane was formed from the organic impurities incorporated in the bulk or adsorb on the surface of TiO_2 and not from the $^{13}CO_2$. We also showed that irradiation of noble metals modified TiO_2 in the atmosphere containing 600 ppm of CO_2 in N_2, leads to an increase in the concentration of both CO_2 and CH_4 in the first stage of reaction followed by further decrease in concentration of methane. This may indicate that observed methane formation results from two competitive processes: (1) methane formation from carbon impurities incorporated into TiO_2 structure or adsorbed at the photocatalysts surface, and (2) methane decomposition over irradiated TiO_2. Moreover, the theoretical calculation of methane concentration in the gas phase, based on amount of incorporated carbon, indicated that in laboratory scale process, amount of methane formed from impurities could be significant and can falsify results regarding eventual CO_2 photoconversion. Thus, careful analysis of the applied photocatalysts is essential for the further reveal of the chemical pathway of CO_2 photoconversion as well as to prove that the artificial photosynthesis can occur.

Acknowledgements

The authors thank Dr. Hab. Eng. Bożena Zabiegała for a valuable advice and student Maciej Kalinowski for assistance during the research. This research was financially supported by the National Centre for Research and Development (strategic program: *Advanced Technologies for Energy Generation*. Task 4: *Elaboration of Integrated Technologies for the Production of Fuels and Energy from Biomass, Agricultural Waste and other Waste*).

References

[1] D. Liu, Y. Fernández, O. Ola, S. Mackintosh, M. Maroto-Valer, Ch.M.A. Parlett, A.F. Lee, J.C.S. Wu, Catal. Commun. 25 (2012) 78–82.
[2] K. Koci, L. Obalova, L. Matejova, D. Placha, Z. Lacny, J. Jirkovsky, O. Solcova, Appl. Catal. B: Environ. 89 (2009) 494–502.
[3] X. Yang, T. Xiao, P.P. Edwards, Int. J. Hydrogen Energy 36 (2011) 6546–6552.
[4] K. Koci, L. Mateju, S. Obalova, Z. Krejcikova, D. Lacny, L. Placha, A. Capek, O. Hospodkovad, Solcova, Appl. Catal. B: Environ. 96 (2010) 239–244.
[5] M.A. Asi, C. He, M. Su, D. Xia, L. Lin, H. Deng, Y. Xiong, R. Qiu, X.-Z. Li, Catal. Today 175 (2011) 256–263.
[6] D. Kong, J. ZiangYie Tan, F. ang, J. Zeng, X. Zhang, Appl. Surf. Sci. 277 (2013) 105–110.
[7] J. Mao, L. Ye, K. Li, X. Zhang, J. Liu, T. Peng, L. Zan, Appl. Catal. B: Environ. 144 (2014) 855–862.
[8] J.Z.Y. Tan, Y. Fernández, D. Liu, M. Maroto-Valer, J. Bian, X. Zhang, Chem. Phys. Lett. 531 (2012) 149–154.
[9] L. Collado, P. Jana, B. Sierra, J.M. Coronado, P. Pizarro, D.P. Serrano, V.A. de la Pena O'Shea, Chem. Eng. J. 224 (2013) 128–135.
[10] L. Liu, D.T. Pitts, H. Zhao, C. Zhao, Y. Li, Appl. Catal. A: Gen. 467 (2013) 474–482.
[11] L. Liu, F. Gao, H. Zhao, Y. Li, Appl. Catal. B: Environ. 134–135 (2013) 349–358.
[12] M. Tahir, N.S. Amin, Biochem. Eng. J. 230 (2013) 314–327.
[13] M.T. Merajin, S. Sharifnia, S.N. Hosseini, N. Yazdanpour, J. Taiwan Inst. Chem. Eng. 44 (2013) 239–246.
[14] Q. Zhang, T. Gao, J.M. Andino, Y. Li, Appl. Catal. B: Environ. 123–124 (2012) 257–264.
[15] C. Wang, R.L. Thompson, J. Baltrus, Ch. Matranga, J. Phys. Chem. Lett. 1 (2010) 48–53.
[16] X. Li, H. Pana, W. Li, Z. Zhuang, Appl. Catal. A: Gen. 413–414 (2012) 103–108.
[17] X. Li, Z. Zhuanga, W. Li, H. Pana, Appl. Catal. A: Gen. 429–430 (2012) 31–38.
[18] Y. Li, W.-N. Wang, Z. Zhan, M.-H. Woo, Ch.-Y. Wuc, P. Biswas, Appl. Catal. B: Environ. 100 (2010) 386–392.
[19] L. Chen, M.E. Graham, G. Li, D.R. Gentner, N.M. Dimitrijevic, K.A. Gray, Thin Solid Films 517 (2009) 5641–5645.
[20] Ch.-Ch. Lo, Ch.-H. Hung, Ch.-S. Yuan, J.-F. Wu, Solar Energy Mater. Solar Cells 91 (2007) 1765–1774.
[21] S.S. Tan, L. Zou, E. Hu, Catal. Today 115 (2006) 269–273.

[22] G.R. Dey, A.D. Belapurkar, K. Kishore, J. Photochem. Photobiol. A: Chem. 163 (2004) 503–508.
[23] Y. Ku, W.-H. Lee, W.-Y. Wang, J. Mol. Catal. A: Chem. 212 (2004) 191–196.
[24] S.N. Habisreutinger, L. Schmidt-Mende, J.K. Stolarczyk, Angew. Chem. Int. Ed. 52 (2013) 7372–7408.
[25] K. Koci, L. Obalova, Z. Lacny, Chem. Papers 62 (2008) 1–9.
[26] B. Mei, A. Pougin, J. Strunk, J. Catal. 306 (2013) 184–189.
[27] Q.-H. Zhang, W.-D. Han, Y.-J. Hong, J.-G. Yu, Catal. Today 148 (2009) 335–340.
[28] C. Zhao, A. Krall, H. Zhao, Q. Zhang, Y. Li, Int. J. Hydrogen Energy 37 (2012) 9967–9976.
[29] O. Ola, M. Maroto-Valer, D. Liu, S. Mackintosh, C.-W. Lee, J.C.S. Wu, Appl. Catal. B: Environ. 126 (2012) 172–179.
[30] B. Michalkiewicz, J. Majewska, G. Kadziołka, K. Bubacz, S. Mozia, A.W. Morawski, J. CO_2 Utiliz. 5 (2014) 47–52.
[31] L. Matejova, K. Koci, M. Reli, L. Capek, V. Matejka, O. Solcova, L. Obalova, Appl. Surf. Sci. 285P (2013) 688–696.
[32] K. Koci, L. Matejova, M. Reli, L. Capek, V. Matejka, Z. Lacny, P. Kustrowski, L. Obalova, Catal. Today 230 (2014) 20–26.
[33] X. Li, Z. Zhuang, W. Li, H. Pan, Appl.Catal. A: Gen. 429–430 (2012) 31–38.
[34] T. Yui, A. Kan, C. Saitoh, K. Koike, T. Ibusuki, O. Ishitani, Appl. Mater. Interfaces 3 (2011) 2594–2600.
[35] C.-C. Yang, J. Vernimmen, V. Meynen, P. Cool, G. Mul, J. Catal. 284 (2011) 1–8.
[36] X. Li, Z. Zhuanga, W. Li, H. Pan, Appl. Catal. A: Gen. 429–430 (2012) 31–38.
[37] C.-C. Yang, Y.-H. Yu, B.v.d. Linden, J.C.S. Wu, G. Mul, J. Am. Chem. Soc. 132 (2010) 8398–8406.
[38] A. Cybula, J. Priebe, M.-M. Pohl, J.W. Sobczak, M. Schneider, A. Zielińska-Jurek, A. Brückner, A. Zaleska, Appl. Catal. B: Environ. 152–153 (2014) 202–211.
[39] A. Zielińska-Jurek, A. Zaleska, Catal. Today 230 (2013) 181–187.
[40] E. Kowalska, O.O.P. Mahaney, R. Abe, B. Ohtani, Phys. Chem. Chem. Phys. 12 (2010) 2344–2355.
[41] A. Zielińska, E. Skwarek, A. Zaleska, M. Gazda, J. Hupka, Procedia Chem. 1 (2009) 1560–1566.
[42] Z. Jiang, T. Xiao, V.L. Kuznetsov, P.P. Edwards, Philos. Trans. Royal Soc. A 368 (2010) 3343–3364.
[43] S.N. Habisreutinger, L. Schmidt-Mende, J. Stolarczyk, Angew. Chem. Int. Ed. 52 (2013) 7372–7408.
[44] Y. Izumi, Coord. Chem. Rev. 257 (2013) 171–186.
[45] N. Sobana, K. Selvam, M. Swaminathan, Sep. Purif. Technol. 62 (2008) 648–653.